

**Provided for non-commercial research and education use.  
Not for reproduction, distribution or commercial use.**



**This article appeared in a journal published by Elsevier. The attached copy is furnished to the author for internal non-commercial research and education use, including for instruction at the author's institution and sharing with colleagues.**

**Other uses, including reproduction and distribution, or selling or licensing copies, or posting to personal, institutional or third party websites are prohibited.**

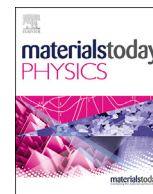
**In most cases authors are permitted to post their version of the article (e.g. in Word or Tex form) to their personal website or institutional repository. Authors requiring further information regarding Elsevier's archiving and manuscript policies are encouraged to visit:**

**<http://www.elsevier.com/authorsrights>**



Contents lists available at ScienceDirect

Materials Today Physics

journal homepage: <https://www.journals.elsevier.com/materials-today-physics>

## Giant enhancement of superconductivity in arrays of ultrathin gallium and zinc sub-nanowires embedded in zeolite



B. Zhang<sup>a</sup>, J. Lyu<sup>a</sup>, A. Rajan<sup>a</sup>, X. Li<sup>b</sup>, X. Zhang<sup>b</sup>, T. Zhang<sup>a</sup>, Z. Dong<sup>a</sup>, Jie Pan<sup>a</sup>, Y. Liu<sup>b</sup>, J. Zhang<sup>b</sup>, R. Lortz<sup>a,\*\*\*</sup>, Z. Lai<sup>b,\*\*</sup>, P. Sheng<sup>a,\*</sup>

<sup>a</sup> Department of Physics, Hong Kong University of Science and Technology, Clear Water Bay, Kowloon, Hong Kong, China

<sup>b</sup> Division of Physical Sciences and Engineering, King Abdullah University of Science and Technology (KAUST), Thuwal 23955-6900, Saudi Arabia

### ARTICLE INFO

#### Article history:

Received 20 June 2018

Received in revised form

2 August 2018

Accepted 8 August 2018

#### Keywords:

Nanowire arrays

Superconductivity

Zeolites

AFI

### ABSTRACT

We have fabricated superconducting samples comprising gallium (Ga) or zinc (Zn) infiltrated into the one-dimensional (1D) linear channels of AlPO-5 (AFI) zeolite, which have an internal pore diameter of 7 Å and are separated by an insulating wall of ~7–9 Å. The Angstrom-scale Ga and Zn sub-nanowires, arranged in Josephson-coupled triangular arrays with an *ab*-plane lattice constant of 14.4 Å, display bulk superconductivity with  $T_c$  values of 7.2 K and 3.7 K, respectively, which are significantly enhanced by a factor of 7 and 4 compared with their bulk values. While the zeolite template of our composite superconductor dictates the nanostructure of Ga and Zn to be 1D in the electronic sense with a highly advantageous effect for the superconducting pairing, the arrangement in a densely packed array structure avoids the shortcomings of other typical 1D superconductors, in which the coherence is usually completely suppressed by strong phase fluctuations.

© 2018 The Authors. Published by Elsevier Ltd. This is an open access article under the CC BY license (<http://creativecommons.org/licenses/by/4.0/>).

Nanotechnology can tailor the structure of materials in such a way that their characteristics change dramatically. Nanostructuring superconductors can cause unusual effects not known from bulk materials. Examples are the oscillating superconducting transition temperature as a function of the film thickness in Pb films [1] or size-dependent breakdowns of superconductivity, e.g. in Al nanowires [2]. In quasi-zero dimensional fine nanoparticles or nanogranular materials of Ga [3,6,7], In [4,5], and Tl [4], enhancements of the superconducting transition temperature were reported. Enhancements in the critical field and temperature were also observed in quasi-one-dimensional (1D) Pb [8–11] and Sn [12,13] nanostructures.

Quasi-1D superconductors are formed by superconducting materials confined in a 1D geometry with a lateral dimensionality smaller than the superconducting coherence length. These materials can be realized either in the form of free-standing individual nanowires or as arrays of parallel nanowires. The latter is found in form of atomic chains in some intrinsic quasi-1D superconductors

such as  $\text{Ti}_2\text{Mo}_6\text{Se}_6$  [14] or  $\text{Sc}_3\text{CoC}_4$  [15]. In addition, arrays of parallel superconducting nanowires have been realized in the pores of mesoporous materials such as SBA-15 silica [8]. Of particular interest are regular, closely spaced arrays of superconducting nanowires, as they can take advantage of quantum confinement and finite size effects within the nanostructure, while some bulk macroscopic superconducting properties such as zero resistance and a measurable Meissner screening effect within the array are maintained by the Josephson coupling between the elements [8,12,16]. While one-dimensionality can have a positive effect on the superconducting parameters, the serious disadvantage is that if the diameter of the nanowire is smaller than the superconducting coherence length, the Mermin-Wagner-Hohenberg theorem [17,18] predicts the suppression of any long-range-ordered physical state by thermal fluctuations. This is because phase-slips in 1D superconducting systems can generate phase changes of  $2\pi$  across a core region of reduced superconducting condensate, resulting in finite resistance at finite temperatures [19–22]. However, if the Josephson coupling between the 1D superconducting elements is strong enough, a three-dimensional long-range-ordered state can result, as predicted from theory [23–26] and verified by experiments [14,16]. The critical parameter for achieving this long-range-ordered bulk phase-coherent superconducting state in the array is the coherence length, and it has been shown, for example, that

\* Corresponding author.

\*\* Corresponding author.

\*\*\* Corresponding author.

E-mail addresses: [lortz@ust.hk](mailto:lortz@ust.hk) (R. Lortz), [zhiping.lai@kaust.edu.sa](mailto:zhiping.lai@kaust.edu.sa) (Z. Lai), [sheng@ust.hk](mailto:sheng@ust.hk) (P. Sheng).

the crossover in 5-nm NbN nanowire arrays in SBA-15 silica is missing due to its particularly short coherence length, while it exists in Pb nanowires in SBA-15 with identical geometric arrangement [27]. To take advantage of the enhancing effect, it is therefore crucial to select superconducting materials with long coherence lengths, as they occur in elemental superconductors. Only then can a nanostructured superconductor in the technical sense with zero resistance be achieved. While zero-resistance phase-coherent states have actually been reported in nanowire arrays, they are usually only found at very low temperatures far below  $T_c$  and in small applied magnetic fields.

In this article, we push the limit of Ga and Zn nanowires to the sub-nanometer range and explore a completely new regime in which Cooper pairs are confined in only a few 100 pm thick wires. The “sub-nanowires” almost approach the limit of a monoatomic chain and are very close to each other: embedded in the linear pores of zeolite single crystals, they form a regular array of almost crystalline quality. Bulk Ga and Zn are well-known elemental BCS (Bardeen–Cooper–Schrieffer) superconductors. Nanostructured Ga and Zn superconductors have already been investigated, but only in sizes ranging from a few nanometers to several tens of nanometers. Using zeolite as a template, we have produced Ga and Zn nanowire arrays on the Angstrom-scale. The advantage of using the zeolite template for the Ga and Zn nanostructures is that the zeolite pores are periodically ordered with a precision that can only be the result of a molecular structure. The specific zeolite we used was the  $\text{AlPO}_4\text{-5}$  (AFI) with linear channels along the  $c$ -axis, with an inner diameter of 0.74 nm and arranged in a triangular lattice with a center-to-center distance of 1.37 nm in the  $ab$  plane. These micro AFI crystallites were synthesized by the hydrothermal method [21]. They are perfect hexagonal platelets with a thickness of  $\sim 2$   $\mu\text{m}$  and lateral dimensions of 4–7  $\mu\text{m}$ . The  $c$ -axis is perpendicular to the lateral plane of the platelet crystals. The AFI crystals are electrically insulating and optically transparent from ultraviolet to near-infrared and thermally stable up to 1200  $^\circ\text{C}$ . To our knowledge, the infiltrated Ga and Zn nanowires in AFI are the thinnest metal nanowires ever produced. Their superconducting characteristics were delineated by using DC (zero frequency) magnetization and specific heat measurements.

## Results and discussion

### Zeolite template characterization

The AFI framework consists of alternating tetrahedral  $(\text{AlO}_4)^-$  and  $(\text{PO}_4)^+$  groups that form linear channels along the  $c$ -axis. As shown in Fig. 1, the AFI crystals have a triangular lattice structure in the  $ab$  plane. The as-made AFI zeolite contains precursors in its pores. They were first burned in an atmospheric environment at 800  $^\circ\text{C}$ . To infiltrate Ga or Zn into the empty pores, we first immerse the platelet crystals with liquid Ga and then heat them to 80  $^\circ\text{C}$  while simultaneously exerting a pressure up to  $\sim 100$  bar in a sealed container. For Zn, we similarly mix Zn powder with AFI crystallites and heat them to 500  $^\circ\text{C}$ . A similar pressure of up to  $\sim 100$  bar was applied. Then, we quenched the AFI crystals containing liquid metals by immersion into liquid nitrogen. The final sample is a solid mixture of AFI crystallites embedded either in solid Ga or Zn and hereinafter referred to as Ga@AFI and Zn@AFI. Since transport measurements are not possible with such samples due to the short circuit through the metal as well as the poor contact between the metallic matrix and the nanowires, we use DC magnetization and specific heat measurements to characterize the superconducting behavior.

It is remarkable that the oxygen atoms lining the wall of the AFI channels can be the reason why liquid Ga and Zn can overcome their surface tension and penetrate into the pores of AFI crystals

under moderate pressure, whereas Sn and Bi, for example, cannot. For Ga and Zn the electronegativity is 1.81 and 1.65, respectively, therefore they have a greater difference to the electronegativity of oxygen, 3.44, than Sn and Bi. From the liquid inlet pressure  $P_E = \frac{4\gamma\cos\theta}{d}$ , where  $d$  denotes the pore size,  $\gamma = 720.4 \text{ mNm}^{-1}$  is the liquid Ga metal's surface tension in the air, and  $\theta$  is the contact angle, one can estimate that  $\theta$  must be very close to  $\pi/2$ , or the liquid would not be able to enter the pores.

### DC magnetization

Fig. 2a shows the zero-field-cooled (ZFC) and field-cooled (FC) DC magnetization of Ga@AFI measured with a VSM SQUID magnetometer. A clear Meissner effect is observed with onset at 7.7 K in a magnetic field of 20 Oe. The superconducting transition is sharp and the transition temperature is  $\sim 7$  times higher than that of bulk Ga ( $T_c = 1.08$  K). In contrast to the observed sharp transition, the 1D nature of free-standing Ga nanowires would be expected to lead to a rather broad transition due to the phase slips. The observed sharp transition must therefore be due to the Josephson coupling between the nanowires. The ZFC data reveal the flux expulsion and subsequent flux treading as the temperature rises. The FC data show only partial flux expulsion. The ZFC and FC data indicate that macroscopic screening currents can be formed in Ga-nanowire arrays embedded in the insulating AFI crystals, which require transverse tunneling current between the Ga nanowires via the Josephson coupling. Fig. 2b shows the magnetization hysteresis loops at different temperatures. Bulk Ga is a well-known type I superconductor with critical field  $H_c = 58$  Oe. Here, however, the Ga nanowire arrays show the typical behavior of a type II superconductor. The initial branch of the hysteresis loops first displays the almost linear behavior of the Meissner state before it passes through a minimum and then very slowly approaches the upper critical field ( $H_{c2}$ ) at about 700 Oe at 1.8 K. The critical field of Ga@AFI is thus more than 100 times higher than that of bulk Ga due to the effect of nanostructuring, which drives the superconductor from type I to type II.

It should be noted that in Fig. 2a, both the ZFC and FC curves have a small shoulder at 6 K, well below  $T_c$ . This shoulder behavior is typical for Josephson arrays [28] and are also often found in quasi-1D superconductors consisting of arrays of atomic chains or nanowires [14,15]. Here, it may well be due to the existence of inhomogeneity within the arrays structure. The lower temperature transition may then simply be due to the increase in the coherence length at lower temperature, whereby those sample areas that were previously separately by greater distances than the higher temperature values of the coherence length and therefore remained incoherent are combined to form a coherent whole.

The DC magnetization data of Zn@AFI are shown in Fig. 3. In Fig. 3a, both the ZFC and FC curves show a sharp Meissner effect below 3.7 K. Compared with the bulk Zn ( $T_c = 0.85$  K), the superconducting transition temperature of Zn@AFI is increased by a factor of 4. The  $M$  versus  $H$  diagram for the Zn nanowires at different temperatures is shown in Fig. 3b. The shape of these hysteresis curves differ significantly from Ga@AFI, and the transition at the critical field is much sharper. As we will demonstrate later with the help of specific heat data, this is due to a type I nature. The fact that the critical field transition appears quite broad is therefore not due to an intermediate Abrikosov vortex phase, but to the large demagnetization factor of the sample. At 1.8 K, the critical field reaches 22 mT, which is approximately four times the value of the bulk Zn ( $H_c = 5.8$  mT).

### Specific heat

The specific heat of Ga@AFI and Zn@AFI was measured with our dedicated home-made calorimeter [27,29]. We analyze the

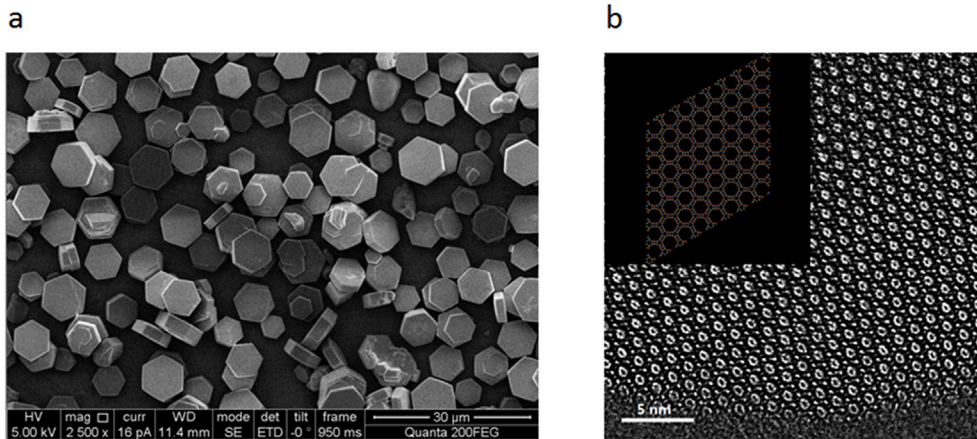


**Fig. 1.** The microstructure of AlPO-5 (AFI) crystals. (a) SEM (scanning electron microscope) image of 5–10  $\mu\text{m}$  platelet AFI crystals with a thickness of  $\sim 2 \mu\text{m}$ . (b) High resolution TEM (transmission electron microscope) image of the AFI crystals with pore size of 0.74 nm.

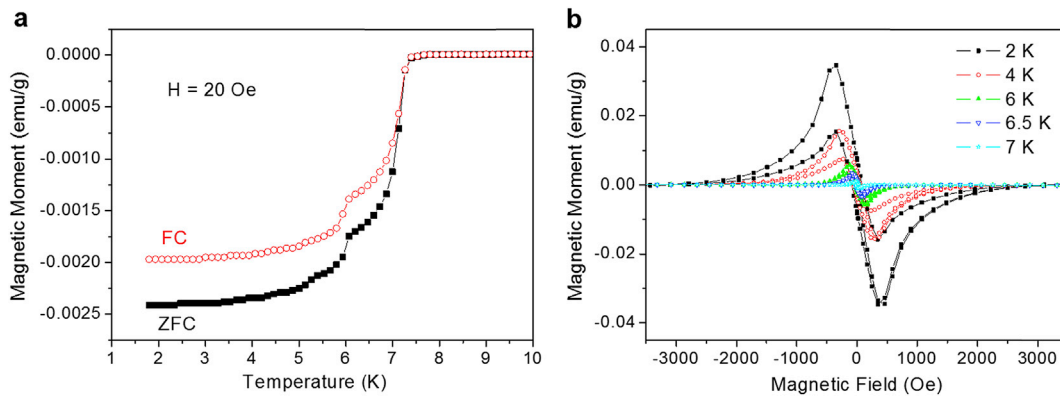


**Fig. 2.** DC magnetization of Ga@AFI. (a) Magnetic moment as a function of temperature for an external magnetic field of 20 Oe under zero-field-cooled and field-cooled conditions. (b) Magnetization hysteresis loops at different temperatures.

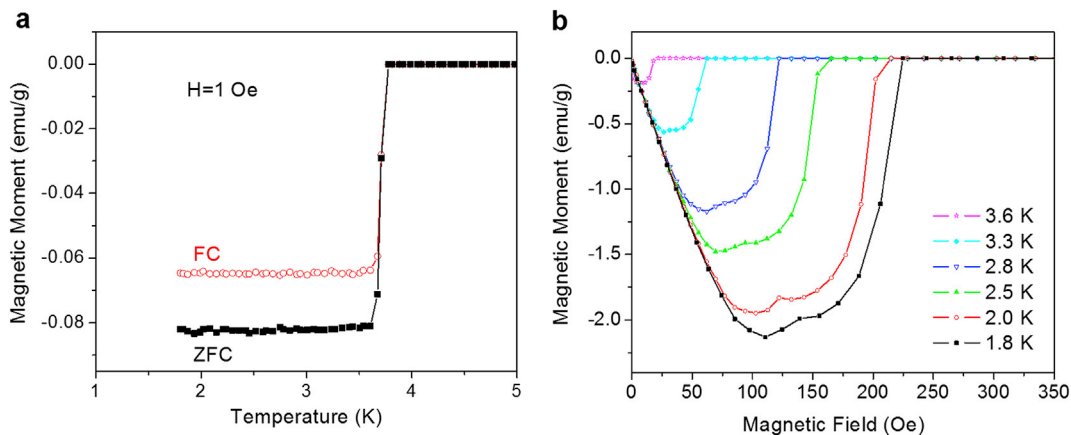


**Fig. 3.** DC magnetization of Zn@AFI. (a) The zero-field-cooled (ZFC) and field-cooled (FC) magnetic moment. (b) Magnetization hysteresis loops at different temperatures.

specific heat in the normal state in the standard approach:  $C_n(T \rightarrow 0) = \gamma_n T + \sum \beta_{2k+1} T^{2k+1}$ . Here the first term, is the electronic contribution of Ga@AFI (or Zn@AFI) with the Sommerfeld constant  $\gamma_n$ . It is denoted by  $C^{elect}$  below. The second term is the low-temperature expansion of the lattice specific heat according to the Debye model. We can obtain the electronic contribution using a magnetic field strong enough to suppress

superconductivity in the nanowires. The specific heat jump associated with the superconductivity will be denoted in the following by  $\Delta C$ . Fig. 4 shows  $C^{elect}/T$  of Ga@AFI (Fig. 4a) and Zn@AFI (Fig. 4b). We can see the superconducting transition anomaly  $\Delta C$ , which is surprisingly sharp for both samples considering the quasi-1D nature of these composites. For Ga@AFI, the transition midpoint is at 7 K, but with a fluctuation tail up to

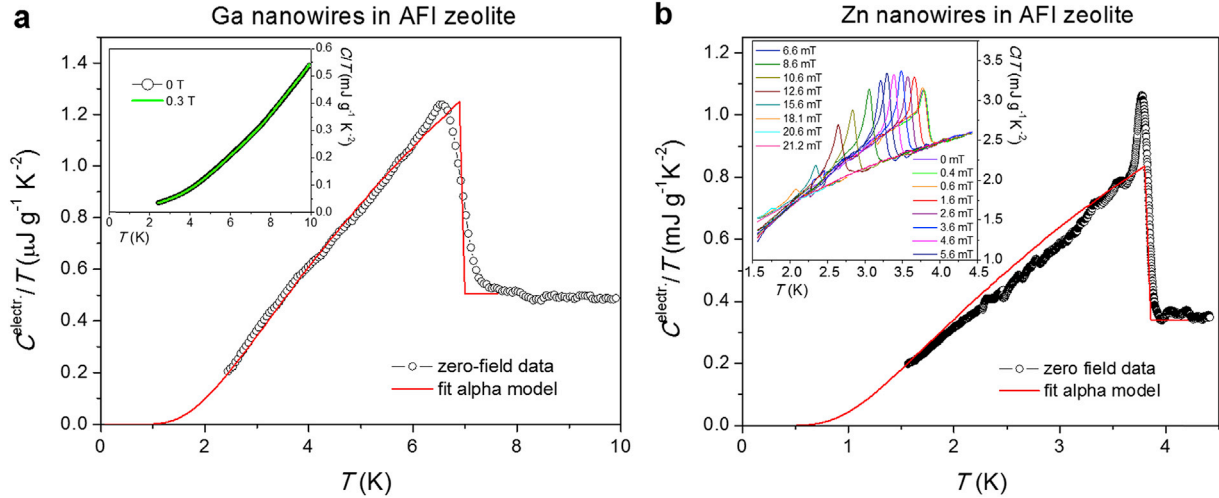


**Fig. 4.** The specific-heat data for Ga@AFI and Zn@AFI. (a) The electronic specific heat of Ga@AFI together with a fit to the alpha model (see text for details). The insert shows the total specific heat in 0 and 0.3 T, which represents the superconducting and normal state, respectively. The superconducting contribution represents only 0.3% of the total specific heat and is not visible without subtraction of the phonon background. (b) The electronic specific heat of Zn@AFI together with a fit to the alpha model. The insert shows the total specific-heat in different applied magnetic fields. The peaks are due to the characteristic first-order nature of this type-I superconductor in finite magnetic fields.

7.7 K. For Zn@AFI, the midpoint occurs at 3.86 K. This is in good agreement with the results of the magnetization.

It is obvious that the superconducting contribution to the specific heat of the Ga nanowires is extremely low.  $\Delta C$  represents only 0.3% of the total specific heat. Despite the enormous  $T_c$  enhancement, these Ga nanowires in AFI zeolite are therefore not suitable for applications due to the very low filling factor of the zeolite pores. Nevertheless, it is amazing how sharp the superconducting transition is and that the composite material can still produce a significant Meissner effect.

The situation is completely different with Zn nanowire arrays. The superconducting transition anomaly  $\Delta C$  of Zn@AFI represents 25% of the total specific heat of the composite material and is therefore clearly visible in the total specific heat without the need to subtract background data. This means that Zn@AFI has a very high pore filling factor, and the nanowires form a homogeneous and very dense array. The Josephson coupling between the wires is so strong that the sample remains a type I superconductor, as can be seen by the sharp peaks sitting on top of the specific heat jumps at  $T_c$ . This is typical for type I superconductors [30], where the superconducting transition becomes of a first-order nature in any finite magnetic field. Although we have carefully tried to compensate for the residual magnetic field in our superconducting magnet cryostat, the peak does not vanish when approaching zero field, which is most likely due to the Earth's magnetic field, which in Hong Kong is almost perpendicular to the axis of our superconducting magnet and hence cannot be compensated.

For a standard BCS superconductor, the BCS theory predicted that  $\frac{\Delta C}{\gamma_n T_c} = 1.43$  and  $\frac{2\Delta_0 k_B}{T_c} = 3.53$ . For Ga@AFI, from the specific-heat, we obtain  $\frac{\Delta C}{\gamma_n T_c} = 1.48$  and  $\frac{2\Delta_0 k_B}{T_c} = 3.6$ , where  $2\Delta_0$  is the full BCS superconducting gap at zero temperature. For bulk Ga, we have  $\frac{\Delta C}{\gamma_n T_c} = 1.44$  and  $\frac{2\Delta_0 k_B}{T_c} = 3.52$ , where  $\frac{2\Delta_0 k_B}{T_c}$  was obtained from a fit with the single-band alpha model [31]. These results indicate that Ga@AFI is still a BCS superconductor despite nanostructuring. However, the electron-phonon coupling in Ga@AFI is somewhat stronger than that of bulk Ga, as indicated by the measured  $\frac{\Delta C}{\gamma_n T_c} = 1.48 > 1.44$ , where  $\gamma_n T_c = 1.44$  is the BCS value. Similarly, for Zn@AFI, we get  $\frac{\Delta C}{\gamma_n T_c} = 1.54$  and  $\frac{2\Delta_0 k_B}{T_c} = 3.6$  while for bulk Zn  $\frac{\Delta C}{\gamma_n T_c} = 1.15$  and  $\frac{2\Delta_0 k_B}{T_c} = 3.2$ . The superconductivity of nanostructured Zn therefore

also has a BCS character. We also see that the electron-phonon coupling in Zn@AFI is slightly enhanced, as indicated by  $\frac{\Delta C}{\gamma_n T_c} = 1.54$ , which is greater than the BCS value of  $\frac{\Delta C}{\gamma_n T_c} = 1.15$ .

#### Superconducting phase diagrams

The superconducting phase diagrams for Ga@AFI and Zn@AFI are shown in Fig. 5. The diagrams are derived from the magnetization data and for Zn@AFI also from the specific heat. Ga@AFI shows the characteristic magnetization hysteresis loops of a type II superconductor. Hence, we derived the temperature dependence of the upper critical field  $H_{c2}(T)$  from the onset of the Meissner signal in the  $M(T)$  data, and from  $M(H)$  (Fig. 5a). A fit to the standard Werthamer, Helfand and Hohenberg (WHH) model [32] was used to extrapolate the upper critical field to zero temperatures to obtain  $H_{c2}(0) = 800$  mT. The model fits well with the data, except at high temperatures, where the data deviate toward higher temperatures. According to the specific heat, this is due to the fluctuation tail above the superconducting main transition at 7 K. The lower critical field  $H_{c1}$  is normally obtained from the first deviation point from a linear behavior of the initial branch of the  $M(H)$  hysteresis loops. This happens with very low magnetic fields of  $\sim 3$  mT at 2 K, and the simple expression  $H_c(T)/H_{c0} = 1 - (T/T_c)^2$  from the Ginzburg-Landau theory was used to extrapolate the data to zero temperature to obtain  $H_{c1}(0) = 3.2$  mT. Note that the latter  $H_{c1}(0)$  determination is not very accurate and should only provide a rough estimate.

Zn@AFI could be identified as type I superconductor from the specific heat data. We determine the temperature dependence of the critical field as the upper onset of a Meissner effect in the  $M(H)$  data, and from the  $T_c(H)$  value in the specific heat, which was determined from the centers of the specific heat jumps that occur just above the peaks. The data agree with the expression  $H_c(T)/H_{c0} = 1 - (T/T_c)^2$  from the Ginzburg-Landau theory sufficiently well to determine  $H_c(0) = 26.4$  mT.

#### Discussion

We have observed an enormous increase in the superconducting transition temperature for both the Ga and Zn sub-

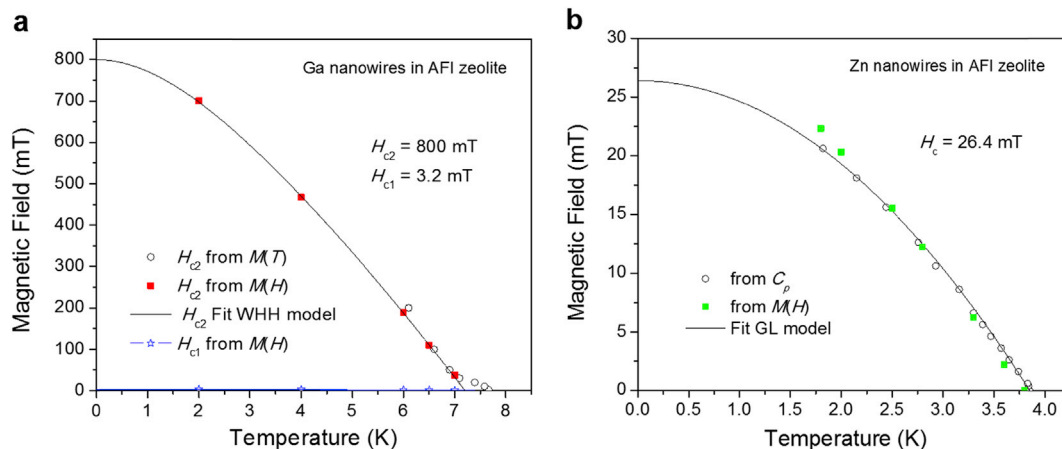


**Fig. 5.** The superconducting phase diagrams of Ga@AFI (a) and Zn@AFI (b). In (a) a fit with the standard Werthamer, Helfand and Hohenberg (WHH) model for the upper critical field of a type II superconductor was added [32] and in (b) a fit with the standard Ginzburg-Landau model for the critical field of a type I superconductor.

nanowires in the linear pores of AFI zeolite single crystals. While the  $T_c$  enhancements are certainly caused by the confinement in the nanostructure, it is remarkable that both composites show characteristics known only from bulk materials, including a sharp superconducting transition and a distinct Meissner effect.

When the size of a conductor is reduced to the Angstrom scale, both the electron and the lattice characteristics can be greatly modified. With the support of AFI templates, Ga and Zn nanowires may form metastable structures that should not be stable in the free-standing form.  $T_c$  enhancements in low-dimensional superconductors are known [3–7,10,11] but are rarely as strong as what we are observing here. Several factors must be considered to explain them. Granular superconductors show enhancements in their superconducting properties [33–38], and in fact a  $T_c$  enhancement of up to 6.4 K in granular Ga was reported [3]. While we believe that our nanowires are most likely of crystalline quality, the arrangement in Josephson-coupled arrays is similar to the coupled grains in granular superconductors, and therefore, similar mechanisms may apply. Various mechanisms have been proposed: it has been demonstrated that quantization of electron motion can have a beneficial effect on  $T_c$  in thin superconducting layers [39] and in small isolated superconducting grains [35]. For very small Sn nanoparticles, the so-called “shell effect” caused by the discretization of energy levels was attributed to significant enhancements in the superconducting gap [40]. The importance of coupling of superconducting nanostructures in granular materials was investigated both experimentally [41] and theoretically [42], and it was shown that in weakly coupled nanograins,  $T_c$  can be increased as a function of decreasing coupling strength [41]. Further mechanisms consider an increased electron-phonon coupling at the surface of nanostructures [43] or the curvature of the surface in cylindrical nanowires [44]. Finally, superconducting nanowire arrays were also considered as a realization of “superstripes”, in which the inclusion of 1D superconducting elements in superlattices was predicted to cause a strong  $T_c$  improvement [45–47]. It must be pointed out that without such positive effects for the Cooper pairing, the  $T_c$  of a superconductor should rather be reduced in small dimensions [14,15,48].

For our 1D sub-nanowire arrays embedded in the zeolite matrix, two further important effects have to be considered. The BCS theory [49] tells us that the transition temperature of a superconductor is determined by  $k_B T_c = 1.13 \hbar \omega_D \exp(-1/N(0)V)$ , where  $\hbar \omega_D$  is the Debye temperature,  $N(0)$  the density of state at the Fermi level, and  $V$  is the electron-phonon coupling. Normally, compared with bulk

metals, the free-standing metal nanowires should have a lower Debye temperature owing to the many soft modes of the thin wire. However, the Ga@AFI and Zn@AFI may have higher Debye temperatures if we consider them as a composite, in which the soft modes are suppressed by the rather rigid AFI pores. This is because AFI has a much higher Debye temperature than either Ga or Zn. It is also remarkable that a high-pressure phase of Ga with a different crystal structure reaches a  $T_c$  value of 7.5 K [50], which is more or less identical to the  $T_c$  value of our Ga@AFI. It is thus likely that our Ga nanowires have a crystalline structure that differs from the bulk at ambient pressure. Another effect that probably applies to our 1D Ga and Zn sub-nanowires is the existence of multiple van Hove singularities in their electronic density of states. Besides a high Debye temperature, a high electronic density of states at the Fermi energy is the second ingredient for high transition temperatures in the BCS  $T_c$  formula. If the Fermi level of the nanowires is at or near a van Hove singularity, their electronic density of states is significantly increased. These elements may account for the enhanced  $T_c$ , while it is the dense array structure with a strong Josephson coupling between the wires that prevents the occurrence of phase slips events and thus stabilizes a state of global phase coherence throughout the array. Only the latter can explain the observation of a sharp specific heat transition, a pronounced Meissner effect and the preserved type I superconductor behavior in Zn@AFI.

Our ultra-thin sub-nanowire arrays in the nanocomposite materials Ga@AFI and Zn@AFI therefore represent a promising approach for the realization of novel “bulk” superconductors with improved superconducting parameters. For Ga@AFI, this approach appears unfortunately limited by the low filling factor of the AFI pores, as the tiny specific heat anomaly demonstrates. However, Zn@AFI shows a very large superconducting transition anomaly in the specific heat, which is characteristic of a very high pore filling factor.

## Conclusions

In this article, we report on the investigation of Ga nanowire and Zn nanowire arrays fabricated using AFI zeolite templates with a pore size of 0.74 nm. To our knowledge, these are the thinnest metal sub-nanowires ever produced. In both cases, we observe huge enhancements of the superconducting transition temperatures compared with the bulk values. We speculate on the source of the  $T_c$  enhancement being due to the increased electronic density of states in the 1D structures with their van Hove singularities, as well

as in the effect of the rigid AFI pore walls, which may significantly increase the Debye temperature of the metal nanowires embedded in the pores. In addition, it is likely that the crystalline structure of the 1D nanowires differs from the bulk and is more advantageous for electron-phonon coupling.

## Experimental section

### Fabrication of Ga@AFI and Zn@AFI

The micro-platelet AFI zeolites with linear channels were used as templates for the fabrication of Ga and Zn nanowires. We synthesized the AFI crystals using the hydrothermal method as described in detail in Reference [21]. The ingredients used in the synthesis were aluminum oxide, phosphorus pentoxide, silicon dioxide, and triethanolamine. The liquid Ga (or Zn) was embedded in the AFI under high pressure up to 100 bar at 80 °C (or 500 °C for Zn) in a sealed container and rapidly cooled in liquid nitrogen. Finally, we obtained Ga@AFI and Zn@AFI.

### Magnetic characterization

The magnetization of Ga@AFI and Zn@AFI was measured with a commercial Quantum Design Vibrating-Sample SQUID magnetometer under ZFC and FC condition in an applied magnetic field of 20 Oe for Ga nanowires and 1 Oe for Zn nanowires. In further field sweep experiments, the temperature was set in the range from 1.8 to 7 K.

### Specific-heat characterization

We have used a homemade calorimeter that can be used in both long relaxation mode and modulated temperature AC mode [29,51]. While the AC technique provides the ultra-high resolution required to detect the tiny electronic signal of nanowires in the insulating zeolite matrix, the relaxation technique is used to determine the absolute value of heat capacity with an accuracy of 1% of the total specific heat. To remove the background signal from AFI and some bulk Ga and Zn residues on the AFI surface, a slightly higher magnetic field than the critical field value was applied, and the resulting normal state data were used to separate the non-superconducting background contribution.

## Acknowledgments

The authors thank Walter Ho and Ulf Lampe for their help. This project is supported by the Research Grants Council of Hong Kong grant RGC 16304314 and the collaborative grant KAUST18SC01 and URF1/3435. R. L. wishes to acknowledge the support of grants SBI17SC14 and IEG16SC03.

## References

- [1] Y. Guo, Y.F. Zhang, X.Y. Bao, T.Z. Han, Z. Tang, L.X. Zhang, W.G. Zhu, E. Wang, Q. Niu, Z. Qiu, Superconductivity modulated by quantum size effects, *Science* 306 (2004) 1915–1917.
- [2] M. Zgirski, K.P. Riikonen, V. Touboltsev, K. Arutyunov, Size dependent breakdown of superconductivity in ultranarrow nanowires, *Nano Lett.* 5 (2005) 1029–1033.
- [3] E. Charnaya, C. Tien, K. Lin, C. Wur, Y.A. Kumzerov, Superconductivity of gallium in various confined geometries, *Phys. Rev. B* 58 (1998) 467.
- [4] J. Watson, Transition temperature of superconducting indium, thallium, and lead grains, *Phys. Rev. B* 2 (1970) 1282.
- [5] W.H. Li, C. Yang, F. Tsao, S. Wu, P. Huang, M. Chung, Y. Yao, Enhancement of superconductivity by the small size effect in nanoparticles, *Phys. Rev. B* 72 (2005) 214516.
- [6] K. Ohshima, T. Fujita, Enhanced superconductivity in layers of Ga fine particles, *J. Phys. Soc. Jpn.* 55 (1986) 2798–2802.
- [7] J. Hagel, M. Kelemen, G. Fischer, B. Pilawa, J. Wosnitza, E. Dormann, H. v. Löhneysen, A. Schnepf, H. Schnöckel, U. Neisel, Superconductivity of a crystalline Ga 84-cluster compound, *J. Low Temp. Phys.* 129 (2002) 133–142.
- [8] M. He, C.H. Wong, P.L. Tse, Y. Zheng, H. Zhang, F.L. Lam, P. Sheng, X. Hu, R. Lortz, “Giant” enhancement of the upper critical field and fluctuations above the bulk  $T_c$  in superconducting ultrathin lead nanowire arrays, *ACS Nano* 7 (2013) 4187–4193.
- [9] J. Wang, Y. Sun, M. Tian, B. Liu, M. Singh, M.H. Chan, Superconductivity in single crystalline Pb nanowires contacted by normal metal electrodes, *Phys. Rev. B* 86 (2012), 035439.
- [10] J. Wang, X. Ma, S. Ji, Y. Qi, Y. Fu, A. Jin, L. Lu, C. Gu, X. Xie, M. Tian, Magnetoresistance oscillations of ultrathin Pb bridges, *Nano Res.* 2 (2009) 671–677.
- [11] J. Wang, X.C. Ma, L. Lu, A.Z. Jin, C.Z. Gu, X. Xie, J.F. Jia, X. Chen, Q.K. Xue, Anomalous magnetoresistance oscillations and enhanced superconductivity in single-crystal Pb nanobelts, *Appl. Phys. Lett.* 92 (2008) 233119.
- [12] Y. Zhang, C.H. Wong, J. Shen, S.T. Sze, B. Zhang, H. Zhang, Y. Dong, H. Xu, Z. Yan, Y. Li, Dramatic enhancement of superconductivity in single-crystalline nanowire arrays of Sn, *Sci. Rep.* 6 (2016) 32963.
- [13] Y.J. Hsu, S.Y. Lu, Y.F. Lin, Nanostructures of Sn and their enhanced, shape-dependent superconducting properties, *Small* 2 (2006) 268–273.
- [14] B. Bergk, A. Petrović, Z. Wang, Y. Wang, D. Salloum, P. Gougeon, M. Potel, R. Lortz, Superconducting transitions of intrinsic arrays of weakly coupled one-dimensional superconducting chains: the case of the extreme quasi-1D superconductor  $Tl_2Mo_6Se_6$ , *N. J. Phys.* 13 (2011), 103018.
- [15] M. He, D. Shi, P.L. Tse, C.H. Wong, O. Wybranski, E.-W. Scheidt, G. Eickerling, W. Scherer, P. Sheng, R. Lortz, 1D to 3D dimensional crossover in the superconducting transition of the quasi-one-dimensional carbide superconductor  $Sc_3CoC_4$ , *J. Phys. Condens. Matter* 27 (2015), 075702.
- [16] Z. Wang, W. Shi, H. Xie, T. Zhang, N. Wang, Z. Tang, X. Zhang, R. Lortz, P. Sheng, I. Sheikin, Superconducting resistive transition in coupled arrays of 4 Å carbon nanotubes, *Phys. Rev. B* 81 (2010) 174530.
- [17] N.D. Mermin, H. Wagner, Absence of ferromagnetism or antiferromagnetism in one- or two-dimensional isotropic Heisenberg models, *Phys. Rev. Lett.* 17 (1966) 1133–1136.
- [18] P.C. Hohenberg, Existence of long-range order in one and two dimensions, *Phys. Rev.* 158 (1967) 383.
- [19] J.S. Langer, V. Ambegaokar, Intrinsic resistive transition in narrow superconducting channels, *Phys. Rev.* 164 (1967) 498–510.
- [20] D. McCumber, B. Halperin, Time scale of intrinsic resistive fluctuations in thin superconducting wires, *Phys. Rev. B* 1 (1970) 1054.
- [21] B. Zhang, Y. Liu, Q. Chen, Z. Lai, P. Sheng, Observation of high  $T_c$  one dimensional superconductivity in 4 Å carbon nanotube arrays, *AIP Adv.* 7 (2017), 025305.
- [22] W. Shi, Z. Wang, Q. Zhang, Y. Zheng, C. Jeong, M. He, R. Lortz, Y. Cai, N. Wang, T. Zhang, Superconductivity in bundles of double-wall carbon nanotubes, *Sci. Rep.* 2 (2012) 625.
- [23] B. Stoeckly, D. Scalapino, Statistical mechanics of Ginzburg-Landau fields for weakly coupled chains, *Phys. Rev. B* 11 (1975) 205.
- [24] K. Kobayashi, D. Stroud, Theory of fluctuations in a network of parallel superconducting wires, *Phys. C* 471 (2011) 270–276.
- [25] R. Klemm, H. Gutfreund, Order in metallic chains. II. Coupled chains, *Phys. Rev. B* 14 (1976) 1086.
- [26] P. Lee, T. Rice, R. Klemm, Role of interchain coupling in linear conductors, *Phys. Rev. B* 15 (1977) 2984.
- [27] C.H. Wong, F.L.Y. Lam, J. Shen, M. He, X. Hu, R. Lortz, The role of the coherence length for the establishment of global phase coherence in arrays of ultra-thin superconducting nanowires, *Supercond. Sci. Technol.* 30 (2017), 105004.
- [28] G. Carapella, P. Sabatino, C. Barone, S. Pagano, M. Gombos, Current driven transition from Abrikosov-Josephson to Josephson-like vortex in mesoscopic lateral S/S’ superconducting weak links, *Sci. Rep.* 6 (2016) 35694.
- [29] H.K. Mak, P. Burger, L. Cevey, T. Wolf, C. Meingast, R. Lortz, Thermodynamic observation of a vortex melting transition in the Fe-based superconductor  $Ba_{0.5}K_{0.5}Fe_2As_2$ , *Phys. Rev. B* 87 (2013), 214523.
- [30] Y. Wang, R. Lortz, Y. Paderno, V. Filipov, S. Abe, U. Tutsch, A. Junod, Specific heat and magnetization of a  $ZrB_{12}$  single crystal: characterization of a type II/1 superconductor, *Phys. Rev. B* 72 (2005), 024548.
- [31] H. Padamsee, J.E. Neighbor, C.A. Shiffman, Quasiparticle phenomenology for thermodynamics of strong-coupling superconductors, *J. Low Temp. Phys.* 12 (1973) 387.
- [32] N.R. Werthamer, E. Helfand, P.C. Hohenberg, Temperature and purity dependence of the superconducting critical field,  $H_{c2}$ . III. Electron spin and spin-orbit effects, *Phys. Rev.* 147 (1966) 295–302.
- [33] A. Shalnikov, Superconducting thin films, *Nature* 142 (1938), 74–74.
- [34] W. Buckel, R. Hilsch, Supraleitung und Widerstand von Zinn mit Gitterstörungen, *Z. Physik* 131 (1952) 420–442.
- [35] B. Abeles, R.W. Cohen, G.W. Cullen, Enhancement of superconductivity in metal films, *Phys. Rev. Lett.* 17 (1966) 632–634.
- [36] R.W. Cohen, B. Abeles, G.S. Weisbarth, Strong-coupling superconductivity in gallium, *Phys. Rev. Lett.* 18 (1967) 336.
- [37] B. Abeles, R.W. Cohen, W.R. Stowell, Critical magnetic fields of granular superconductors, *Phys. Rev. Lett.* 18 (1967) 902–905.
- [38] R.W. Cohen, B. Abeles, Superconductivity in granular aluminum films, *Phys. Rev.* 168 (1968) 444–450.
- [39] C.J. Thompson, J.M. Blatt, Shape resonances in superconductors – II simplified theory, *Phys. Lett.* 5 (1963) 6–9.

- [40] S. Bose, A.M. García-García, M.M. Ugeda, J.D. Urbina, C.H. Michaelis, I. Brihuega, K. Kern, Observation of shell effects in superconducting nanoparticles of Sn, *Nat. Mater.* 9 (2010) 550–554.
- [41] U.S. Pracht, N. Bachar, L. Benfatto, G. Deutscher, E. Farber, M. Dressel, M. Scheffler, Enhanced cooper pairing versus suppressed phase coherence shaping the superconducting dome in coupled aluminum nanograins, *Phys. Rev. B* 93 (R) (2016) 100503.
- [42] J. Mayoh, A.M. García-García, Strong enhancement of bulk superconductivity by engineered nanogranularity, *Phys. Rev. B* 90 (2014) 134513.
- [43] V.L. Ginzburg, On surface superconductivity, *Phys. Lett.* 13 (1964) 101–102.
- [44] C.H. Wong, R. Lortz, Edge effect and significant increase of the superconducting transition onset temperature of 2D superconductors in flat and curved geometries, *Phys. C* 521–522 (2016) 50–54.
- [45] A. Perali, A. Bianconi, A. Lanzara, N.L. Saini, The gap amplification at a shape resonance in a superlattice of quantum stripes: a mechanism for high  $T_c$ , *Solid State Commun.* 100 (1996) 181–186.
- [46] A. Bianconi, A. Valletta, A. Perali, N.L. Saini, High  $T_c$  superconductivity in a superlattice of quantum stripes, *Solid State Commun.* 102 (1997) 369–374.
- [47] A. Bianconi, A. Valletta, A. Perali, N.L. Saini, Superconductivity of a striped phase at the atomic limit, *Phys. C* 296 (1998) 269–280.
- [48] T. Sekihara, R. Masutomi, T. Okamoto, Magnetic-field-independent superconductivity of ultrathin Pb films on cleaved GaAs surface, *J. Phys.: Conf. Ser.* 456 (2013), 012034.
- [49] J. Bardeen, L.N. Cooper, J.R. Schrieffer, Microscopic theory of superconductivity, *Phys. Rev.* 106 (1957) 162.
- [50] S.V. Vonosovsky, Yu A. Izumov, E.Z. Kurmaev, *Superconductivity of Transition Metals*, Springer-Verlag, Berlin-Heidelberg, New York, 1982.
- [51] P.F. Sullivan, G. Seidel, Steady-state, ac-temperature calorimetry, *Phys. Rev.* 173 (1968) 679–685.